

# ELASTO-DYNAMIC BEHAVIOR OF A 2D SQUARE LATTICE WITH ENTRAINED FLUID

V. Dorodnitsyn\*, A. Spadoni†

\* École Polytechnique Fédérale de Lausanne  
CH-1015 Lausanne  
Switzerland  
e-mail: vladimir.dorodnitsyn@epfl.ch

† École Polytechnique Fédérale de Lausanne  
CH-1015 Lausanne  
Switzerland  
e-mail: alex.spadoni@epfl.ch

**Key words:** Wave propagation, cellular solids, band structure, fluid-structure interaction, dispersion relation

**Abstract.** Numerical investigation of wave propagation in a cellular solid with closed cells configuration and entrained fluid showed an existence of two types of pressure waves, which have opposite polarization and have different phase and group velocities. This is in agreement with the Biot's theory, unless that the slow pressure wave appears beyond the first resonant frequency of the skeleton members. In order to explain this fact we propose an analytical macro-mechanical model and study dynamical modes contribution.

## 1 INTRODUCTION

The dynamics of cellular materials present a number of unique phenomena not found in solid, single-phase materials. Elastic wave propagation in cellular solids is an active topic of current research. Classical approach to describe wave propagation in porous solids is based on Biot's theory [1, 2, 3]. However this theory requires mechanical properties of both drained and undrained conditions, which are often not available analytically, and comparisons with specific configurations are based on experiments [4, 5]. Nevertheless, this model remains a benchmark which was validated with rigorous micromechanical models [6, 7, 8, 9]. The bulk elastic properties of cellular solids can be found from several methods [10, 11], however they are done for statics and do not allow to analyze elastic wave propagation and dispersion sources.

Based on analysis of a periodic square lattice system as a prototypical two-phase medium [12, 13], we expand our studies to explain the behavior of slow pressure wave,

which appears beyond a certain frequency. Two pressure waves were predicted by Biot [1, 2] within the same frequency range (range of coexistence), whereas our results show that second pressure wave does not propagate below the first resonant frequency of the skeleton member.

Moreover, Biot's theory is based on complex expressions of geometric and material parameters which does not allow the analysis of the physical origin of specific wave-propagation characteristics. In this paper, we propose a much simpler model for macro-mechanical model which explains physically the dynamic behavior of cellular solid with closed cell configuration and entrained gas.

## 2 NUMERICAL ANALYSIS

We find two types of pressure waves, which have opposite polarization and have different phase velocities [13]. This is in agreement with the Biot's theory, unless that the slow pressure wave appears beyond the first resonant frequency of the skeleton members. This phenomenon is verified by our numerical model based on finite element analysis where the element type is chosen according to relative density value [12]. The unit cell correspondent to this problem is briefly described in the next section.

### 2.1 Unit cell model

We employ a periodic square lattice in plane conditions with fluid-filled cells as a two-phase medium (Fig. 1a,b) with the unit out-of-plane thickness. Therefore, the RVE (Fig. 1c) can be defined by the characteristic length  $L$  and wall thickness  $h/2$ . The lattice

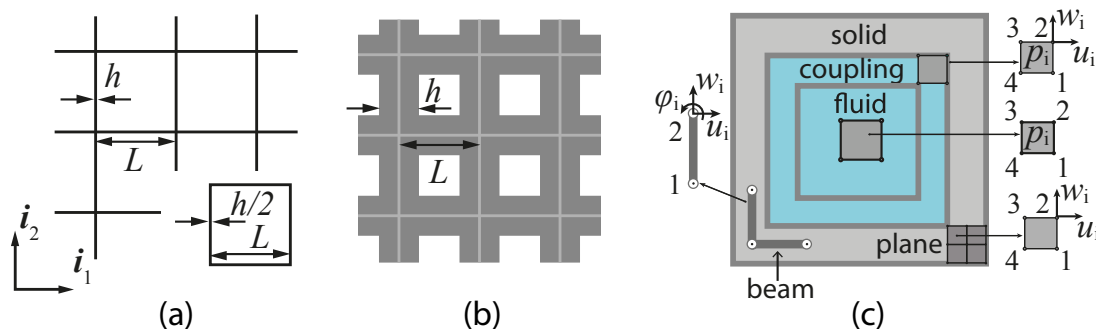


**Figure 1:** Square lattice with walls thickness  $h$  and cell length  $L$  with (a)  $\rho^* < 30\%$  and (b)  $\rho^* > 30\%$ . The superposed unit cell in (a) has thickness  $h$ . RVE with solid portion discretized (c) by either beam or 4-node plane elements shown with appropriate degrees of freedom:  $u_i, w_i$  displacement dofs for both types of elements, and rotational dof ( $\phi_i$ ) for beam elements only. In both cases, coupling elements with both structural and pressure dofs are employed to model fluid-structure interaction.

vectors  $\mathbf{e}_1 = L\mathbf{i}_1$ ,  $\mathbf{e}_2 = L\mathbf{i}_2$  define the periodicity of an infinite medium. We use the results from finite-element (FE) analysis, detailed in [13, 12], where the band structure

(relation between the frequency  $\omega$  and the wavevector  $\mathbf{k} = \{k_x, k_y\}^T$  along the boundaries of the irreducible Brillouin zone [14]) is obtained from the eigenvalue problem

$$([K_r](\mathbf{k}) - \omega^2[M_r](\mathbf{k}))\hat{\mathbf{u}}_r = \mathbf{0}. \quad (1)$$

Here  $[K_r]$  and  $[M_r]$  are the stiffness and mass matrices of the coupled system reduced to take in to account symmetry conditions from Bloch theorem, and  $\hat{\mathbf{u}}_r$  is the nodal degree-of-freedom (dof) vector with displacement and pressure amplitudes. Each eigenvalue  $\omega(\mathbf{k})$  corresponds to a wave mode. For  $L = 100 \mu\text{m}$ ,  $h/L = 0.02$ , skeleton Young's modulus  $E_s = 1 \text{ KPa}$ , density  $\rho_s = 1000 \text{ Kg/m}^3$ , and air as the entrained fluid with speed of sound  $c_0 = 343 \text{ m/s}$ , density  $\rho_f = 1.225 \text{ Kg/m}^3$ , and bulk modulus  $B_f = 142 \text{ KPa}$ , we obtain the band-structure shown in Fig. 2; the solid phase is discretized with beam elements [12]. Following the notation in [12], dashed lines in Fig. 2 denote the solution to the structure-only configuration (simulations with no pressure dofs involved), while solid lines denote the solution to the two-phase (FSI) configuration.

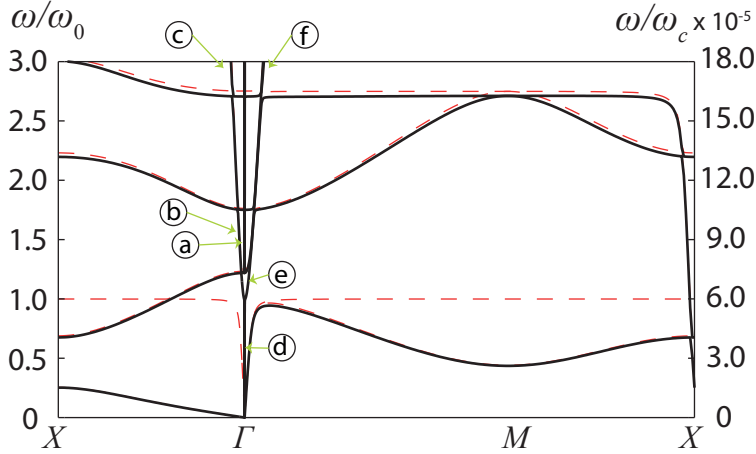


**Figure 2:** Band structure for RVE with  $L = 100 \mu\text{m}$ ,  $\rho^* = 0.04$  discretized with beam elements for the irreducible Brillouin Zone with high-symmetry points  $\Gamma$ ,  $X$ ,  $M$ . Left ordinate is normalized by the first natural frequency of a clamped-clamped beam,  $\omega_0$ ; the second ordinate is normalized by the first natural frequency of the fluid cavity alone,  $\omega_c$ . Solid lines are the solution to the FSI problem, dashed lines are the solution to the structure-only case. Circled letters a-f denote wavenumber combinations used to depict deformed configurations in Fig. 3.

For the aforementioned properties, the following facts transpire. Cell-wall resonance  $\bar{\omega} = \omega/\omega_0 = 1$  is a strong source of dispersion. Note that if  $\rho_f \ll \rho_s$ ,  $\omega_0$  is that of a clamped-clamped beam in vacuum, otherwise the fluid added mass must be included. The shear response is not affected by the entrained fluid for the square lattice. The FSI solution yields a fast pressure mode for  $\bar{\omega} < 1$  and two pressure modes for  $\bar{\omega} > 1$ . Wavemodes corresponding to the labels in Fig. 2 are shown in Fig. 3. The pressure wavemode (a) has the same polarization for  $\bar{\omega} < 1$  and  $\bar{\omega} > 1$ . For  $\hat{\omega} = \omega/\omega_c < 1$ , the

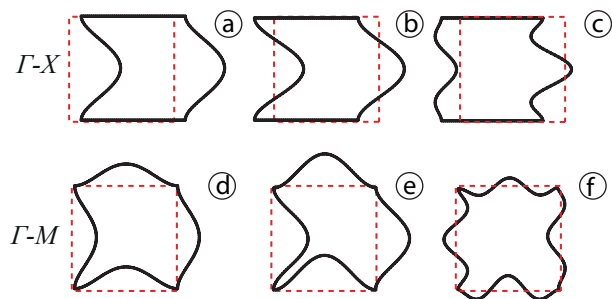


**Figure 3:** Fluid-structure wavemodes corresponding to the wavenumber combinations indicated by the labels a-f in Fig. 2. Solid and dashed lines denote the deformed and initial configurations respectively.

pressure distribution within the pores is uniform and only odd modes of the cell walls are excited.

A study of two pressure wavemodes in  $\Gamma - X$  direction, namely (a) and (b), represents the main topic of the present paper. Specifically, the qualitative shape of the wavemodes allows us to study dynamic behavior in simplified macro-mechanical model (sec. 2.2). One may notice that deformations of two pressure wavemodes are of the same type and polarization but with the different phase and group velocities. The close up comparison of these two wavemodes in the coexistent frequency range is shown in the Fig. 4(a),(b). Fig. 4(a) verifies the fact that two wavemodes differs qualitatively by a rigid body motion shift  $\Delta\phi$ .

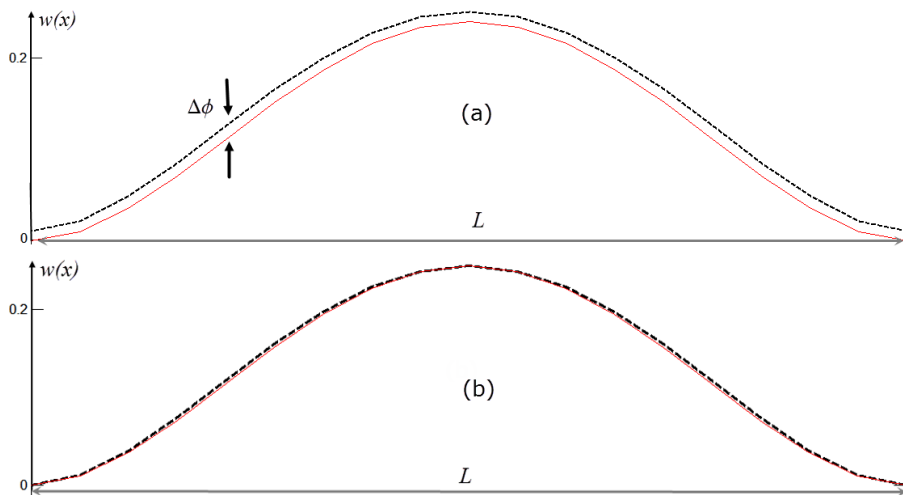


**Figure 4:** A close-up comparison of two pressure wavemodes from Fig. 3. Normalized but not shifted wavemodes are shown in (a), where  $\Delta\phi$  denotes the shift. Wavemodes shifted to the same origin are shown in (b). Red solid line is a fast p-wavemode, and black dashed line is a slow p-wavemode.

One can write the speed of sound in the entrained fluid as  $c_0 = f_c \cdot c_0^{\text{air}}$ , where  $c_0^{\text{air}}$  is a speed of sound in air, and  $f_c$  is a variable factor. Then by changing  $f_c$  from 0.1 to 10, one

obtains the band structures shown in the Fig. 5. I can be mentioned that change of speed

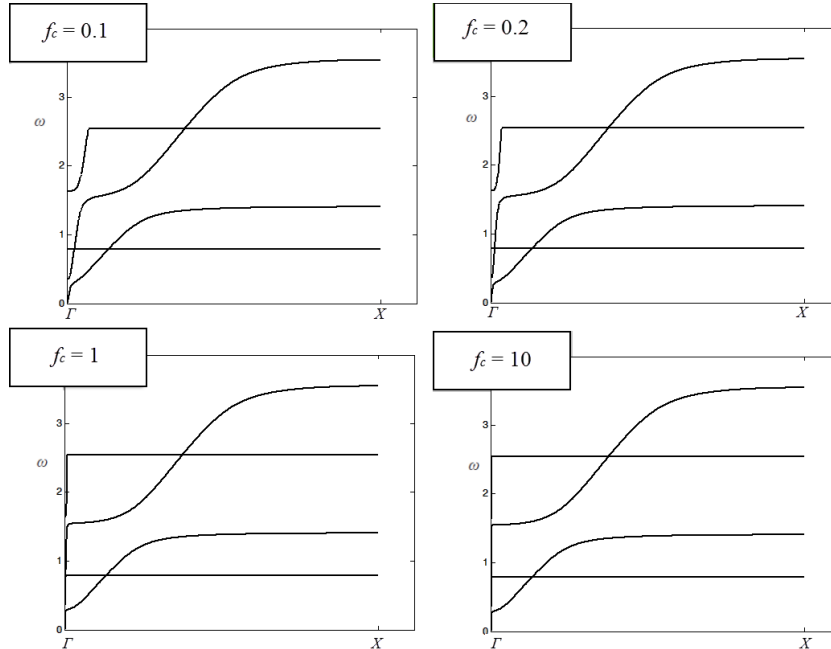


**Figure 5:** Band structure evolution with the growth of speed of sound in the entrained fluid.

of sound in the fluid affects the slow pressure wavemode, whereas it does not influence the fast pressure wavemode at all. Therefore, we preliminary conclude that the fast pressure wavemode is determined by structural components and it is not determined by the fluid.

Further in the paper we consider air as an entrained gas in the cell and we fix the relative density value at  $\rho^* = 0.04$ .

## 2.2 Analytical model

A close-up comparison of two pressure wavemodes in coexistent frequency range (provided by the Fig. 4), and the observation done from the Fig. 5, we propose a macro-mechanical model composed of Euler-Bernoulli beam with an average pressure force  $P_b$  acting on it. The force  $P_b$  is introduced based on the hydrostatic-like behavior of the entrained fluid [13]. The presence of axially displaced solid frame components is given by the boundary condition on the shear force at one of the ends of the beam, say at  $x = 0$ . Effective stiffness of the shear springs is  $\hat{k}$ , which represents the rigidity of the horizontal beam-walls. The other end of the beam is constrained to behave in the same way. The model is shown in the Fig. 6. Consider  $L$  to be the length of the beam, therefore for  $x \in [0, L]$  one can define corresponding transversal displacements  $\hat{w}(x, t)$  which is the function of space and time.

The change in pressure can be described as an external distributed force over the

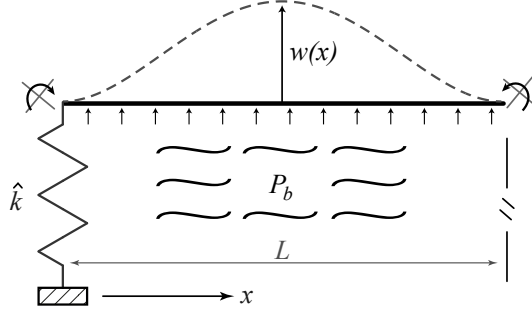


**Figure 6:** Macro-mechanical model with fluid force  $P_b$  and shear spring with effective stiffness  $\hat{k}$ .

beam's face. The difference of volumes resultant from structural displacements creates the pressure gradient, which is a constant in space and can be written as

$$P_b = -\hat{\beta} \frac{\Delta V}{V} = -\frac{\hat{\beta}}{L^2} \int_0^L \hat{w}(x, t) dx. \quad (2)$$

Hence we can write the integro-differential equation of motion with respect to unknown beam's displacement function  $\hat{w}(x, t)$

$$EI \frac{\partial^4 \hat{w}(x, t)}{\partial x^4} + \rho_s A \frac{\partial^2 \hat{w}(x, t)}{\partial t^2} - P_b = \hat{f}(t), \quad (3)$$

where  $\hat{f}(t)$  is a distributed external force applied.

### 2.3 Characteristic equation

If one assumes harmonic motion

$$\hat{w}(x, t) = w(x)e^{i\omega t}, \quad \hat{f}(t) = fe^{i\omega t}, \quad (4)$$

and divides both sides of Eq. (3) on  $EI$ , the governing system becomes

$$w''''(x) - \alpha^4 w(x) + \frac{\hat{\beta}}{EIL^2} \int_0^L w(x) dx = f/EI, \quad (5)$$

where  $\alpha^4 = \omega^2(\rho_s A)/(EI)$ . Eq. (5) can be solved by considering that the is a definite integral with constant limits of integration. Differentiating Eq. (5) by the spatial variable leads to homogeneous fifth-order ODE, whose general solution contains five unknown constants

$$w(x) = C_1 \sin \alpha x + C_2 \cos \alpha x + C_3 \sinh \alpha x + C_4 \cosh \alpha x + C_5. \quad (6)$$

Substituting this solution back into Eq. (5) and assuming  $f = 0$ , one determines one of the constants, say  $C_5$ . Therefore the general solution to Eq. (5) would contain four

constants, and should satisfy to the following four boundary conditions

$$\begin{aligned}
w'(0) &= 0, \\
w'(L) &= 0, \\
w(0) &= w(L), \\
-EIw_1'''(0) &= -\hat{k}w(0),
\end{aligned} \tag{7}$$

which physically mean that we restrict rotations at the ends of each beam, and we couple the shear forces at the ends with transversal displacements through special shear springs characterized by stiffness  $\hat{k}$ . Inducing the boundary conditions Eqs. (7) leads to homogeneous linear system of four equations with four unknowns. In order to have nontrivial solution to the latter system, one has to set the determinant of this system to be zero. The resultant equation is known as characteristic equation, which solution gives the eigenfrequencies of macro-mechanical model. In accordance with Eqs. (5),(7) the characteristic equation in the studied case is

$$\begin{aligned}
&L\alpha(EI L\alpha^4 - \hat{\beta})\hat{k} + L\alpha(-EI L\alpha^4 + \hat{\beta})\hat{k} \cos L\alpha \cosh L\alpha + \\
&(EI L\alpha^4(EI L\alpha^4 - \hat{\beta}) - 2\hat{\beta}\hat{k}) \left[ 2 \sin L\alpha \sinh^2 \frac{L\alpha}{2} + (\cos L\alpha - 1) \sinh L\alpha \right] = 0.
\end{aligned} \tag{8}$$

For a unit cell with  $L = 1$  m,  $h = 0.01$  m,  $E = 1$  KPa, and entrained air, first seven roots are given by Eq. (9) respectfully. The corresponding modeshapes can be found by solving Eqs. (7) for each eigenvalue, which lead to a problem of finding a nullspace of a corresponding characteristic matrix. Since the rank of this matrix is reduced by unity at each eigenvalue, one can find a corresponding modeshape with normalization of resultant displacement function by the free constant. For example, first nonzero modeshape in comparison with the wavemodes from Fig. 4(c) is shown in the Fig. 7.

$$\alpha L_{air} = \left\{ \begin{array}{c} 0 \\ 3.8204 \\ 6.2832 \\ 7.8532 \\ 12.5664 \\ 14.1372 \\ 18.8496 \end{array} \right\} \tag{9}$$

## 2.4 Wave analysis

One can notice that system of Eqs. (5),(7) does not contain the information on the wave propagation. Even though the first modeshape of analytical model is qualitatively

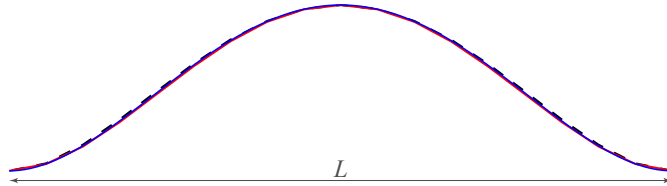


**Figure 7:** Analytical modeshape (blue solid line) with  $\beta$  correspondent to air, in comparison with numerical wavemodes from Fig. 4 (red solid and dashed black lines denote fast and slow p-waves, respectfully). Each modeshape is normalized by quarter of its maximal displacement.

the same as the p-wavemodes from FE model, the wave analysis should be done in order to evaluate dynamical characteristics of the system, such as phase and group velocities of the wave. Our approach would be based on matrices analysis of FE system. Assuming hydrostatic-like behavior of the pressure acting on the surface of the walls, and similarly to the representation of  $P_b$  in Eq. (2), one can rewrite FE stiffness matrix from Eq. (1) as

$$[K] = \begin{bmatrix} K_{11} + \beta\Upsilon & K_{12} - \beta\Upsilon \\ K_{21} - \beta\Upsilon & K_{22} + \beta\Upsilon \end{bmatrix}, \quad (10)$$

which corresponds to the global vector of displacements consists of left and right sides' displacements. Here  $K_{ij}$  is an  $ij$ -minor of correspondent structural stiffness matrix,  $\beta$  is an effective bulk modulus, and  $\Upsilon$  is a matrix full of ones in order to provide an average force. Mass matrix can be represented in the similar way but with no  $\beta$  terms, since fluid acts like an effective spring and contributes stiffness only.

Note that structure only case can be derived from condition  $\beta = 0$ . Denote the correspondent stiffness matrix as  $[K_s]$ . Then, applying symmetry conditions from Bloch theorem and assuming plane harmonic wave, reduced stiffness matrix can be presented in the following form

$$[\tilde{K}_f] = [\tilde{K}_s] + \beta\Upsilon(1 - \cos \mu L) = [\tilde{K}_s] + \hat{\beta}\Upsilon, \quad (11)$$

where

$$\hat{\beta} = \beta(1 - \cos \mu L) \quad (12)$$

is a function of a wavenumber  $\mu$ . Eq. (11) provides the structure of wavenumber contribution to the fsi problem. This let us to introduce an effective bulk modulus for the analytical model from sec. 2.2. An effective stiffness of the shear spring, which represents the rigidity of the wall parallel to the wave propagation direction ( $\Gamma - X$ ), can be written similarly as

$$\hat{k} = k(1 - \cos \mu L) = \frac{EA}{L}(1 - \cos \mu L). \quad (13)$$

Plugging Eqs. (12),(13) back to characteristic equation Eq. (8), one obtains dispersion relation, which relates wavenumber  $\mu$  to the frequency of the coupled system  $\omega$ . It is

worth notice that this dispersion relation is derived in more simple way compared to straightforward approach of applying wave conditions on displacements and forces directly for the analytical model.

Our current state of work is to explain the coexistence of two pressure wavemodes in specific frequency regime by analyzing the resultant dispersion relation. Determining the exact proof of the slow p-wavemode existence condition requires more precise formulation of pressure force representation, namely pressure modes should be treated as an infinite sum of the pressure distributions independent on the structural modes (sec. 7.6 in [15]). The orthogonality of pressure and structural modes is not provided, therefore one has to apply the theory of self adjoint operators in order to treat the expansion theorem [16] in the latter case. This analysis will be uploaded soon.

### 3 CONCLUSION

This article presents modal and wave propagation analysis of analytical unit cell, which is proposed as a macro-mechanical analogy of cellular solid with periodic square lattice. The characteristic equation for an analytical unit cell gives the set of eigenfrequencies, which correspond to the natural frequencies of the coupled fluid-structure interaction problem. It gives physical and mathematical origins to Biot's theory interpretation of a second pressure wave. The modeshape analysis shows the qualitative similarity of wavemodes of fast and slow p-waves to the first nonzero modeshape from the proposed simplified analytical model. Moreover the modal analysis of macro-mechanical model is complemented by the wave analysis, which is built on the detailed study of the equations of motion in the matrix form for the coupled fsi problem. The dispersion relation relates the imposed wavenumber on the system frequency response. The analysis of pressure modes contribution will be added soon.

## REFERENCES

- [1] M. A. Biot, “Theory of propagation of elastic waves in a fluid-saturated porous solid. I. Low-frequency range,” *The Journal of the Acoustical Society of America*, vol. 28, p. 168, 1956.
- [2] M. A. Biot, “Theory of propagation of elastic waves in a fluid-saturated porous solid. II. Higher frequency range,” *The Journal of the Acoustical Society of America*, vol. 28, p. 179, 1956.
- [3] M. A. Biot and D. G. Willis, “The elastic coefficients of the theory of consolidation,” *J. appl. Mech*, vol. 24, no. 4, pp. 594–601, 1957.
- [4] I. Gueven, P. Kurzeja, S. Luding, and H. Steeb, “Experimental evaluation of phase velocities and tortuosity in fluid saturated highly porous media,” *PAMM*, vol. 12, no. 1, pp. 401–402, 2012.
- [5] I. Chekkal, C. Remillat, and F. Scarpa, *High Performance Structures and Materials VI*, ch. Acoustic Properties of Auxetic Foams, pp. 119–130. WIT Press, 2012.
- [6] J. L. Auriault and E. Sanchez-Palencia, “Etude du comportement macroscopique d’un milieu poreux saturé déformable,” *Journal de Mécanique*, vol. 16, no. 4, pp. 575–603, 1977.
- [7] R. Burridge and J. B. Keller, “Poroelasticity equations derived from microstructure,” *The Journal of the Acoustical Society of America*, vol. 70, p. 1140, 1981.
- [8] A. H.-D. Cheng, “Material coefficients of anisotropic poroelasticity,” *International Journal of Rock Mechanics and Mining Sciences*, vol. 34, no. 2, pp. 199–205, 1997.
- [9] F. Chevillotte, C. Perrot, and R. Panneton, “Microstructure based model for sound absorption predictions of perforated closed-cell metallic foams,” *The Journal of the Acoustical Society of America*, vol. 128, p. 1766, 2010.
- [10] F. Chevillotte and R. Panneton, “Elastic characterization of closed cell foams from impedance tube absorption tests,” *The Journal of the Acoustical Society of America*, vol. 122, p. 2653, 2007.
- [11] C. Perrot, F. Chevillotte, and R. Panneton, “Bottom-up approach for microstructure optimization of sound absorbing materials,” *The Journal of the Acoustical Society of America*, vol. 124, p. 940, 2008.
- [12] V. Dorodnitsyn and A. Spadoni, “Elasto-Dynamics of a 2D Square Lattice with Entrained Fluid I: Comparison with Biot’s theory,” *ASME Journal of Vibration and Acoustics*, vol. 136(2), 021024, 2014.

- [13] V. Dorodnitsyn and A. Spadoni, “Elasto-Dynamics of a 2D Square Lattice with Entrained Fluid II: Microstructural and Homogenized Models,” *ASME Journal of Vibration and Acoustics*, 2014, to appear.
- [14] L. Brillouin, *Wave Propagation in Periodic Structures: Electric Filters and Crystal Lattices*. Dover Phoenix Editions, Dover Publications, 2003.
- [15] F. J. Fahy and P. Gardonio, *Sound and Structural Vibration: Radiation, Transmission and Response*. Elsevier Science, 2007.
- [16] L. Meirovitch, *Fundamentals of vibrations*. Waveland Press, 2010.